Global Change Biology

Life after a fiery death: fire and browning effects on dissolved organic matter composition in experimental freshwater ponds

Journal:	*Global Change Biology*
Manuscript ID	GCB-23-0474
Wiley - Manuscript type:	Research Article
Date Submitted by the Author:	02-Mar-2023
Complete List of Authors:	Spiegel, Cody; University of California San Diego, Ecology, Behavior, Evolution Mladenov, Natalie; San Diego State University, Civil Construction & Environmental Engineering Wall, Christopher; University of California San Diego, Ecology, Behavior, Evolution Hollman, Kelly; San Diego State University, Civil Construction & Environmental Engineering Tran, Cindy; University of California San Diego, Ecology, Behavior, Evolution Symons, Celia; University of California Irvine, Ecology and Evolutionary Biology Shurin, Jonathan; University of California San Diego, Ecology, Behavior, Evolution
Keywords:	dissolved organic matter, decomposition, wildfire, fluorescence spectroscopy, mesocosm, brownification, pyrogenic carbon
Abstract:	Drier and hotter conditions linked with anthropogenic climate change increase wildfire frequency and intensity, influencing terrestrial and aquatic carbon cycles at broad spatial and temporal scales. Wildfire destabilizes riparian watersheds surrounding aquatic systems like lakes and ponds that lead to enhanced deposition of terrestrial subsidies, resulting in increased leaching of dissolved organic matter (DOM) from plants, a phenomenon known as “browning.” We tested the effects of browning (quantity of plant biomass) and its interaction with fire (burned vs. unburned plant material) on DOM composition, concentration, and degradation (biological vs. photochemical) in freshwater ponds using a gradient experimental design. Dissolved organic carbon (DOC) concentration increased nonlinearly exceeding 56 mg/L at the highest plant biomass levels in both fire treatments. Fluorescence and ultraviolet-visible light absorbance spectroscopic indices showed nonlinear relationships with DOM chemical composition and plant biomass such as greater humification and specific ultraviolet absorbance at 254 nm (a proxy for aromatic DOM) in the highest biomass levels. The burned plant material showed reduced humification over time compared to unburned demonstrating how fire impacts DOM processing in aquatic ecosystems. DOC decomposition was dependent on the loading of

	detritus as evidenced by the greater loss in DOC due to biodegradation than photodegradation occurring at intermediate biomass levels. Our results reveal that fire and browning elicit nonlinear and interactive responses in the dynamics and composition of DOM in aquatic systems. Our study illuminates how the quantity of plant detritus and its chemical transformation by fire jointly impact its processing and role in aquatic environments.

Life after a fiery death: fire and browning effects on dissolved organic matter composition in experimental freshwater ponds

Cody J. Spiegel[1*], Natalie Mladenov[2], Christopher B. Wall[1], Kelly Hollman[2], Cindy H. Tran[1], Celia C. Symons[3], Jonathan B. Shurin[1]

[1]Ecology, Behavior and Evolution Section, Department of Biological Sciences, University of California, San Diego, CA, USA

[2]Department of Civil Construction & Environmental Engineering, San Diego State University, CA, USA

[3]Department of Ecology and Evolutionary Biology, University of California, Irvine, CA, USA

*corresponding author: cjspiege@ucsd.edu

Keywords: dissolved organic matter, decomposition, wildfire, fluorescence spectroscopy, mesocosm, brownification, pyrogenic carbon

Author contacts: cbwall@ucsd.edu; khollman2052@sdsu.edu; cht010@ucsd.edu; nmladenov@sdsu.edu; csymons@uci.edu; jshurin@ucsd.edu

Fire and browning effects on DOM

Abstract

Drier and hotter conditions linked with anthropogenic climate change increase wildfire frequency and intensity, influencing terrestrial and aquatic carbon cycles at broad spatial and temporal scales. Wildfire destabilizes riparian watersheds surrounding aquatic systems like lakes and ponds that lead to enhanced deposition of terrestrial subsidies, resulting in increased leaching of dissolved organic matter (DOM) from plants, a phenomenon known as "browning." We tested the effects of browning (quantity of plant biomass) and its interaction with fire (burned vs. unburned plant material) on DOM composition, concentration, and degradation (biological vs. photochemical) in freshwater ponds using a gradient experimental design. Dissolved organic carbon (DOC) concentration increased nonlinearly exceeding 56 mg/L at the highest plant biomass levels in both fire treatments. Fluorescence and ultraviolet-visible light absorbance spectroscopic indices showed nonlinear relationships with DOM chemical composition and plant biomass such as greater humification and specific ultraviolet absorbance at 254 nm (a proxy for aromatic DOM) in the highest biomass levels. The burned plant material showed reduced humification over time compared to unburned demonstrating how fire impacts DOM processing in aquatic ecosystems. DOC decomposition was dependent on the loading of detritus as evidenced by the greater loss in DOC due to biodegradation than photodegradation occurring at intermediate biomass levels. Our results reveal that fire and browning elicit nonlinear and interactive responses in the dynamics and composition of DOM in aquatic systems. Our study illuminates how the quantity of plant detritus and its chemical transformation by fire jointly impact its processing and role in aquatic environments.

Fire and browning effects on DOM

Introduction

Wildfires play a major role in global carbon (C) cycles, and are on the rise as climate change makes vegetation more flammable (Halofsky et al. 2020; Harvey and Enright 2022). Geography, antecedent weather conditions, and plant community composition shape regional fire regimes (Bond 2013). The relative significance of these factors for driving trends in fire activity differ greatly across global ecoregions (McKenzie et al. 2004; Bowman et al. 2009). Nonetheless, it is clear that drier and hotter conditions linked with anthropogenic climate change increase wildfire frequency and intensity that influence terrestrial C cycles at broad spatial and temporal scales (Abatzoglou and Williams 2016; Lasslop et al. 2019).

As large-scale ecological disturbances, wildfires can catalyze many forms of ecosystem change. First, fires can trigger landscape shifts such as the replacement of woody vegetation or shrublands with more flammable grasslands (Zedler et al. 1983; D'Antonio and Vitousek 1992; Stevens-Rumann and Morgan 2016). Second, burning can cause rapid C release through combustion which depletes stored C in plant biomass and watersheds (Pellegrini et al. 2015; Cornelissen et al. 2017; Granath et al. 2021), and transforms the chemical properties of organic matter via pyrolysis (limited oxygen) or thermal oxidation (Wang et al. 2015; Ward et al. 2017). Fire can affect plant material by either reducing its availability as a substrate for microbial decomposition, or altering its chemical structure (e.g., by pyrolysis or thermal oxidation) which influences its decomposability (Bowring et al. 2022). Lastly, soil destabilization and hydrophobicity from high severity wildfires leads to accelerated runoff and erosion that can be deposited into streams, rivers, and lakes (Larsen et al. 2009; Lewis et al. 2019). Burned C particulates can persist and bioaccumulate within aquatic ecosystems (Campos and Abrantes

2021; Burton et al. 2022). The ecological effects of wildfire may therefore cross the aquatic-terrestrial boundary.

Despite covering a small fraction of the Earth's surface, biogeochemical activity within lakes is a critical component of the global C cycle (Mulholland and Elwood 1982; Cole et al. 2007). Lake metabolism is regulated by the processing of organic and inorganic material from both internal (autochthonous) production as well as terrestrial (allochthonous) inputs that directly influence trophic dynamics and nutrient cycling. Wildfire destabilizes riparian watersheds surrounding aquatic systems like lakes and ponds that lead to enhanced deposition of terrestrial subsidies, resulting in increased leaching of dissolved organic matter (DOM) from plants, a phenomenon known as “browning” (Kritzberg et al. 2020). Dissolved organic carbon (DOC) from terrestrial sources can lead to net heterotrophy where lake community respiration exceeds internal primary productivity (Hanson et al. 2003), suggesting that allochthonous inputs significantly regulate lake ecosystem function (e.g., Wetzel 1984; Berggren et al. 2022; Fonseca et al. 2022). Allochthonous organic C is either transported to the ocean via hydrological networks, emitted as respired CO_2, or stored in sediments. The amount of C buried annually in lake sediments is comparable to that stored in the ocean via the C pump (Ward et al. 2017). Large disturbances like wildfire may catalyze further browning, and thus rising DOC concentrations, which subsequently affect greenhouse gas emissions, burial in lake sediments or export to the ocean.

As downstream recipients, lakes are especially vulnerable to post-fire erosion and sedimentation, and the deposition of organic subsidies following a fire has the potential to impact DOM processing and storage (Cooper et al. 2015; McCullough et al. 2019). Previous work shows that annual streamflow increases as much as 30% the first year following a fire (Lavabre

et al. 1993). Sampling in response to fire shows increases in post-fire lake DOC in addition to reduced water quality (McEachern et al. 2000; Earl and Blinn 2003; Wagner et al. 2018). By surveying water chemistry in two-year post-fire lakes on Alberta's Boreal Plain, Allen et al. (2003) found that mean DOC concentrations in lake water from burned watersheds was 1.4-fold higher compared to reference watersheds. Yet, variation in the chemical composition of DOM due to the heterogeneity in the vegetation of burned watersheds may determine the fate of allochthonous inputs and their impact on lake productivity and respiration. For instance, other studies observed that post-fire increases in DOC were attributed to autochthonous DOM production (Moody and Martin 2001). The effects of fire on DOM chemistry in aquatic systems remains unclear due to the complex chemical transformations that can occur. Therefore, identifying changes in post-fire DOM chemistry is of great importance as it will provide insight into DOM persistence, fate, and reactivity.

Changes in DOM chemistry can affect reactivity and susceptibility to photochemical and microbial degradation, the two dominant controls on biogeochemical lake C cycling (Wetzel 1984; Morris and Hargreaves 1997; Obernosterer and Benner 2004). Mixtures of burned organic materials (collectively, pyrogenic carbon (PyC)) can significantly influence decomposition rates through alterations to its quality and quantity as well as changes to the aquatic environment that affect light penetration and microbial activity (Pereira et al. 2011; Wang et al. 2015; Santos et al. 2019). For example, aromatic PyC subsidies strongly influence the structure of microbial communities in aquatic environments (Bostick et al. 2021; Chen et al. 2022). Moreover, light absorbing chromophoric DOM compounds also contribute to variation in photo- and biodegradation rates between lakes with different allochthonous inputs from watersheds (Cory et

al. 2007; Laurion and Mladenov 2013; Helms et al. 2013). Thus, fire-induced chemical changes and browning may impact DOM processing in lakes.

In this study, we address the effects of fire and browning on the concentration, composition, and decomposition of DOM in experimental freshwater ponds. Using an array of 30 (400 L) mesocosms with a gradient design of increasing plant biomass, we ask the following: (1) How does fire (burned or unburned plant material) and browning (quantity of plant biomass) affect DOC concentration? (2) How does burning plant material affect DOM chemical composition? and (3) How do microbial activity and photodegradation contribute to DOM decomposition between burned and unburned sources? We predict an increase in DOC concentrations from initial C leaching, but reduced DOC concentrations in the burned ponds due to C depletion from combustion (Pellegrini et al. 2015). We also hypothesize that fire and browning should weaken the photodegradation and microbial decomposition of DOM from the combined effects of increased light attenuation due to shading, reduced dissolved oxygen concentrations at high detrital loading, and greater aromaticity (and therefore reduced lability) from burning. Our study aims to advance knowledge of aquatic DOM dynamics by using a gradient experimental design to detect critical ecosystem thresholds in response to browning and fire.

Materials

Plant material

We selected two California native plant species *Salvia leucophylla* (hereafter, sage) and *Salix lasiolepis* (hereafter, willow) to simulate the effects of terrestrial loading. Sage was chosen due to its wide distribution, growing on arid, sandy, and rocky soils, and common throughout

western North America at elevations from 762 to 3000 m (Keeley and Fotheringham 2001). Willow is a deciduous species found in riparian zones. Both sage and willow occur in fire-prone scrub and woodland ecosystems in California making them appropriate species for this study. Twenty-three sage plants were purchased from a nursery on 9 June, 2021 and transplanted into pots with a sand-vermiculite mixture and grown for 60 days. Willow was harvested from the University of California Dawson Los Monos Reserve in San Diego, CA. Cut stems (~ 1 cm diameter) and leaves from sage and willow branches were placed inside a greenhouse to air dry (24 h). The plant material was then placed in a drying oven at a constant temperature (24 h at 45°C) until dry before being introduced into the mesocosms.

To simulate the effects of fire, a portion of sage and willow was burned in a 75 L aluminum container using a blow torch. To ensure the plant material was not completely combusted, the container's lid was used to regulate oxygen flow and smother the plant material as needed (similar to the "thermal oxidation" and "pyrolysis" conditions defined by Wang et al. 2015). We used visual assessment to divide the plant material into two burn severity groups: low severity (likely pyrolyzed with intact green leaves showing noticeable black burns on the stems and sticks) and high severity (likely thermally oxidized with grey leaves, sticks, and stems including ash) (Figure S1). The two burn severity groups were then combined. All leaves, sticks, and stems were gathered and pooled according to fire treatment. All burned and unburned plant material was packed into separate 25 x 15 cm nylon bags of 250 μm mesh size. Leaf litter bags aided in sinking and containment once added to the mesocosms while also allowing for water flow and grazing of microorganisms and other small invertebrates. In total, each tank received a 1:1 mass ratio of sage and willow to reach the cumulative target mass. After weighing, the nylon bags with plant material were set in a drying oven (24 h at 45°C) before being placed in their

assigned tanks. We recovered the litter bags at the end of the experiment for final mass measurements. All litter bags were removed and oven-dried (7 d at 45°C) and re-weighed. The initial and final masses of sage and willow were used to measure leaf litter decomposition over the course of the experiment.

Mesocosm experimental design

Thirty mesocosms (400 L plastic cattle tanks) filled with freshwater were assembled at the University of California, San Diego Biological Field Station in October of 2021. A plankton mixture collected from Lake Murray and Lake Miramar in San Diego, CA using a vertical tow (64 μm mesh net; 7.6 m depth) was used in equal aliquots (~ 433 mL) to stock mesocosms with resident plankton communities. Tanks were regularly filled with fresh water to replace losses to evaporation. The experimental design was a gradient of plant biomass crossed with a burning treatment, resulting in two 15-tank gradients of plant material that was either burned or unburned. In the gradient design each tank received incremental increases of plant material ranging from 0 g to 400 g with a total of fifteen tanks per plant treatment type (burned vs. unburned). The gradient design allowed us to test for thresholds and nonlinearities in the response of pond ecosystems to terrestrial subsidies. Tanks were filled on 27 December 2021, plankton mixture was added on 1 November 2021, the plant material was added on 5 November, 2021, and the experiment ended on 16 March, 2021.

In situ incubations

To test the roles of photo- and biodegradation on DOC decomposition, we conducted three incubation experiments (Day 10, 30, and 60). The last two experiments on Days 30 and 60

were excluded because positive net changes in DOC were observed in some replicates which indicated potential contamination or methodological issues. The first experiment (initiated on Day 10) is presented and includes the period showing the greatest changes in DOC during the experiment.

Each tank received four 100 mL sealed bags subjected to one of four treatments manipulating the presence of microbes and UV light. A combination of clear and opaque Sterile Whirl-Pak© bags were used to construct UV treatments that transmitted the entire solar spectrum or completely excluded light exposure. 100 mL of water from each tank was collected and filtered (F) through pre-combusted (2 h at 550°C) glass-fiber filters (0.7 μm GF/F; Whatman, Maidstone, UK) to limit but not fully exclude microbial activity; other bags were filled with 100 mL of unfiltered water (UF) that included microbes resident in the tanks. This resulted in four treatment conditions in a 2 x 2 factorial design: UV transmissible-unfiltered [UV-UF]; UV transmissible-filtered [UV-F]; Non-UV transmissible-unfiltered [NoUV-UF]; and Non-UV transmissible-filtered [NoUV-F]. All bags (four per tank x 30 tanks, n = 120) were then secured to 8.8 x 25.4 x 7.6 cm plastic trays and suspended ca. 15 cm below the surface. At the end of the incubation period (7 d; see Dempsey et al. 2020), all bags were removed, filtered through pre-combusted 0.7 μm GF/Fs into muffled (5 h at 550°C) borosilicate amber vials (60 mL), and transported on ice to the Water Innovative and Reuse Lab (WIRLab) at San Diego State University (SDSU).

Filtration is essential for measuring microbial degradation of DOC with studies recommending a 0.45 or 0.2 μm pore size to remove microbiota from samples (Bertilsson and Tranvik 2000; Magyan and Dempsey 2021). Many 0.45 and 0.2 μm filters, however, are composed of organic material such as cellulose acetate, which can induce contamination

problems, leading some researchers to recommend 0.7 μm GF/F filters (Khan and Subramania-Pillai 2006; Denis et al. 2017). The efficiency of filtration to remove microbes and regrowth over the course of the experiment or during storage was not verified during this study.

The UV and filtration treatments were used to distinguish between effects of photodegradation vs. microbial decomposition on DOC loss. The percent change in DOC concentration between the four Whirl-Pak bag treatments and ambient tank conditions yielded effects for individual degradation pathways: 1) photodegradation, 2) microbial degradation, and 3) the combined effect of both photo- and microbial degradation. That is, the percent change in DOC concentration over the seven-day incubation was calculated for each bag in each tank. The photodegradation (or UV-only) effect was indicated by the difference in DOC percent change between the UV-F and NoUV-F, the microbe effect (or micobes-only) was the difference in DOC percent change between the NoUV-UF and NoUV-F, and the combined microbial and photochemical effect (or UV and microbes) was the difference between the UV-UF and NoUV-F.

DOC concentration analysis

DOC concentration was measured at four times: 10, 30, 60, and 120 days after plant addition using an integrated water column sampler (47.6 cm depth). To prepare for concentration analysis, samples were filtered through pre-combusted 0.7 μm GF/Fs into muffled borosilicate amber vials, and then acidified with 37% HCl to a pH of 3. DOC concentration analysis was conducted using a high temperature combustion method (Shimadzu TOC-L Total Organic Carbon Analyzer) in the WIRLab at SDSU. Samples were calibrated with potassium hydrogen phthalate standards (ranging from 1 to 50 mg C/L) and analyzed according to WIRLab standard

protocols with ~ 10% of samples in duplicate. For all duplicated samples, standard deviations were within 10% of mean values; sample results falling outside of this range were either re-analyzed or excluded.

EEM spectral analysis

We used fluorescence EEM data to characterize the chemistry of the compounds that contributed to DOM in the ponds. Water was collected for EEMs analysis and individually filtered from every tank (n = 30) through a 64 μm mesh into 100 mL acid-washed (10% HCl) polypropylene containers. The filter mesh was rinsed with ddH_2O between collections to prevent cross-tank contamination. Samples were filtered into muffled borosilicate amber vials using 0.7 μm GF/Fs, refrigerated (< 24 h) and then transported on ice to the WIRLab for analysis. EEMs measure the excitation and emission wavelengths at which fluorescence occurs to characterize specific molecular structures (Coble 1996). A fraction of chromophores in DOM are fluorescent compounds (Stedmon and Nelson 2015), and certain regions present in the EEMs were used to characterize aspects of the chemical composition in the ponds.

Optical properties, ultraviolet-visible light (UV-vis) absorbance and fluorescence were acquired simultaneously (at room temperature of 21-23 °C) using a Horiba Scientific Aqualog Fluorometer on filtered water samples in a quartz cuvette with a path length of 1 cm. EEMs fluorescence was inner-filter corrected, blank-subtracted and Raman-normalized, and first and second order Rayleigh scatter bands were excised (see Laurion and Mladenov 2013).

Representative tanks of low (5 g), intermediate (125 g), and high biomass (225 g) levels were used to illustrate the compositional shifts in DOM chemistry over the course of the experiment (see Figures S4-S6). The heights of major peaks in the EEMs corresponding to different

molecular structures were identified using the wavelength ranges identified by (Coble 1996, 2007): Peak A (humic-like, λex=~250 nm; λem=380-460 nm), Peak C (humic-like, λex=~405 nm; λem= 490-510 nm), Peak M (marine/microbial humic-like peak, λex=~312 nm; λem=380-420 nm), and Peak B (amino acid-like, λex=~275 nm; λem=~310-320 nm).

Indices generated by UV-vis absorbance and fluorescence spectroscopy.

To classify the DOM chemical characteristics, we calculated three fluorescence indices (Table 1): the humification index (HIX = ratio of areas under the emission curve at 435–480 nm and 300–345 nm plus 435–480 nm at an excitation wavelength 245 nm) that described the degree of humification (high HIX = more terrestrial humic-like material) (Zsolnay et al. 1999), the fluorescence index (FI = emission intensity at 470 nm divided with that of 520 nm at 370 nm excitation) which indicated source material (microbial-precursor FI value ≈ 1.8 or terrestrial-precursor FI ≈ 1.3) (McKnight et al. 2001), and the freshness index (BIX), representing the degree of processed DOM, was calculated as the ratio of emission intensity at 380 nm to the maximum emission intensity between 420 and 435 nm at excitation wavelength 310 nm (Parlanti 2000).

Additionally, we further classified the DOM chemical characteristics by calculating two UV-vis absorbance indices (Table 1): the ratio of the slope (S_R) parameters ($S_{275-295}$:$S_{350-400}$) which is used as a proxy for molecular weight (MW) (Helms et al. 2008) and the specific ultraviolet absorbance at 254 nm ($SUVA_{254}$) to indicate aromaticity (Weishaar et al. 2003).

Fire and browning effects on DOM

Table 1. Descriptions of fluorescence and UV-vis absorbance indices for dissolved organic matter used in this study.

Parameter	Abbreviation	Description	Literature
Specific ultraviolet absorbance at 254 nm	$SUVA_{254}$	Higher absorbance at 254 nm divided by DOC concentration indicates greater aromaticity	Weishaar et al. (2003)
Spectral slope ratio	S_R	Inversely related to the molecular weight	Helms et al. (2008)
Humification index	HIX	Increases with DOM humification	Zsolnay et al. (1999)
Freshness index	BIX	Increases with freshly produced DOM	Parlanti (2000)
Fluorescence index	FI	Higher values indicate the relative contribution of autochthonous vs. allochthonous DOM	McKnight et al. (2001)

Statistical analyses

Fire treatment effects were modeled using general additive models (GAMs) implemented in R's mgcv package (Wood 2017). Flexible smoothers in a GAM framework are well suited to

model the nonlinear responses in our gradient experimental design. Models for each parameter were individually analyzed at the four discrete sampling points since results for a single full model introduced extreme concurvity (> 0.9).

We estimated the effects of fire and browning using separate GAMs with a gaussian error distribution for all response variables. Final models were selected with the lowest generalized cross-validation (GCV) and Akaike Information Criterion scores (see Tables S1-S4), and greatest deviance explained (DE) using backward stepwise selection. Lower GCV scores typically correspond with higher DE indicating that a model minimizes the smoothed predictors while maximizing explanatory power (Wood 2017). In our fitted GAMs, the significance of the smooth plant biomass term is a test of deviation from a flat or null function that is constant at 0 over all observed values of the predictor variable (Wood 2017); deviation from this indicates the presence of a nonlinear pattern. For all fitted models, Wald tests of the significance of each parametric and smooth term were performed. Here, the figures presented show either *two smooths* that indicate a significant nonlinear smooth for each fire treatment, or *one global smooth* (in black) that represents an estimated mean across the covariate plant biomass for both fire treatments (see Results). We used this model selection procedure for all analyses to identify whether browning affected the different response variables, and whether the relationships differed between the fire treatments.

Results

Mesocosm DOC concentration

DOC concentration showed a rapid nonlinear increase with plant biomass 10 days after plant addition that gradually declined in both fire treatments over time (Figure 1). DOC values

ranged from 5.0 to 56.5 mg/L along the plant biomass gradient. Intermediate plant biomass amounts for the burned treatment at 10 days showed about 20% less DOC compared to the unburned treatment as evidenced by the differences between the fitted smooth functions (difference in trends; solid lines) shown in red with approximate 95% confidence intervals (p = 0.005, Figure S2). Averaged across all plant biomass amounts, the burned treatment had an average 8 mg/L less DOC than the unburned treatment. By Day 120, DOC concentrations significantly declined with no significant difference between fire treatments.

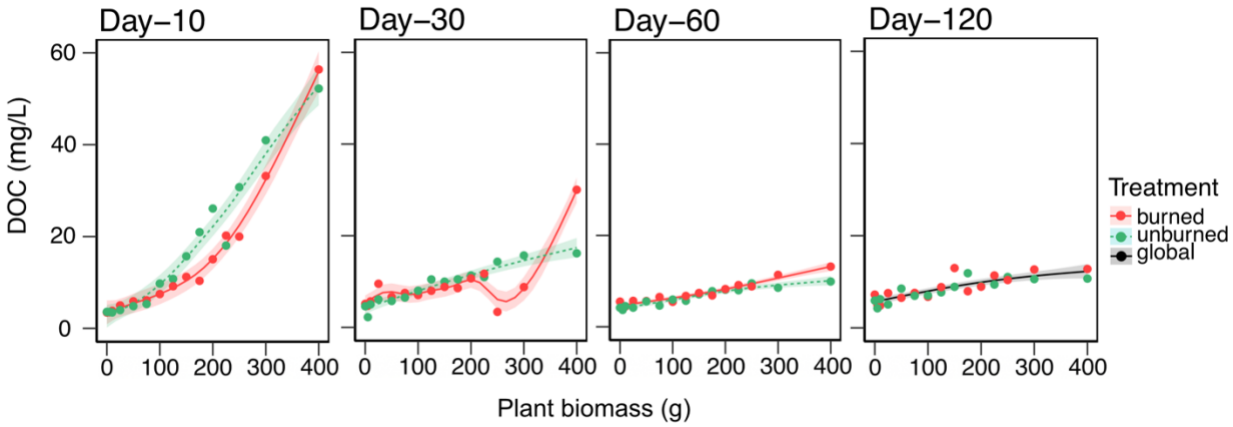

Figure 1. Dissolved organic carbon (DOC) concentrations across plant biomass addition at four discrete sampling points for the burned (red) and unburned (green) treatments. Plots with a single global smooth indicates that a model with one fit line for the burned and unburned treatments best describes the data, while separate smooths for each fire treatment indicate that a model with different fits for the two burning treatments showed best agreement.

Fluorescence and UV-vis absorbance indices

Effects of browning and DOM chemical alterations by fire were observed in the fluorescence (HIX, BIX, and FI) and UV-vis absorbance ($SUVA_{254}$ and S_R) indices, and varied strongly over time. $SUVA_{254}$, an indicator of aromaticity, showed a nonlinear relationship with

plant material at Day 10 with greater aromaticity at intermediate plant biomass amounts for both fire treatments (Figure 2a). The increase in $SUVA_{254}$ persisted over time and was most apparent at Day 60 with a significant difference between fire treatment (p = 0.001). The lower $SUVA_{254}$ values in the burned treatment compared to the unburned treatment at 60 days can be seen by the differences between the fitted smooth functions (difference in trends; solid lines) in red with approximate 95% confidence intervals (Figure S3a). Average across all plant biomass amounts for both fire treatments, $SUVA_{254}$ increased by an average 12.4% by Day 120 relative to Day 10.

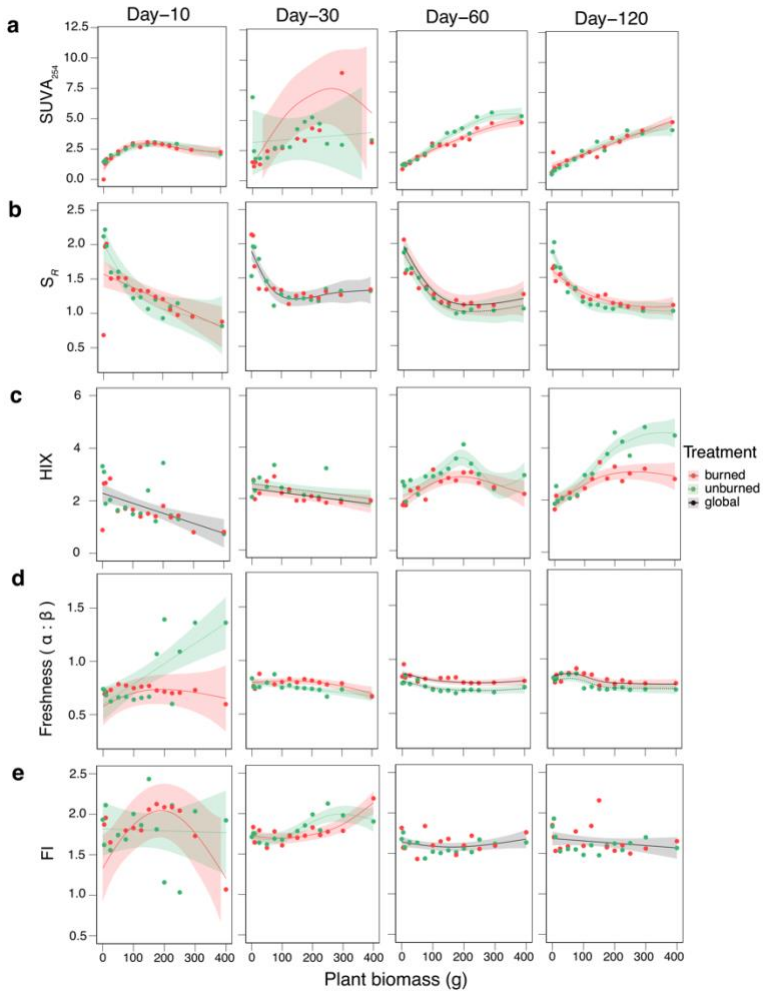

Figure 2. Changes in **a:** $SUVA_{254}$, **b:** spectral slope ratio, **c:** humification index, **d:** freshness index, and **e:** fluorescence index with increasing plant biomass for the burned (red) and unburned (green) treatments. Plots with a single global smooth indicates that a model with one fit line for the burned and unburned

treatments best describes the data, while separate smooths for each fire treatment indicate that a model with different fits for the two burning treatments showed best agreement.

S_R, which has been employed in other studies as a proxy for DOC MW (Helms et al. 2008), showed a negative relationship across the plant biomass gradient at Day 10, which remained consistent over time with no significant differences between the fire treatments (Figure 2b). After Day 30, S_R remained around an average value of 1.0 at intermediate/higher biomass levels, indicating that high MW compounds increased over time.

HIX showed a negative relationship with plant biomass at Day 10 and 30 indicating less humified DOM (Figure 2c). By Day 60, HIX positively increased with a significant effect of fire treatment ($p = 0.0006$) and greater humification in the unburned treatment. By Day 120, the difference between fire treatment remained as evidenced by the differences between the fitted smooth functions (difference in trends; solid lines) shown in red with approximate 95% confidence intervals ($p < 0.0001$, Figure S3c).

There was a significant effect of fire treatment and browning on the BIX index with more recently produced DOM in the unburned treatment at Day 10 ($p = 0.01$, Figure 2d). The trends in freshness stabilized by Day 30 and remained over time with no significant difference between the fire treatments.

The FI index showed a positive, nonlinear trend along the plant biomass gradient, indicating greater microbial sources (average FI value ~ 2.0) at intermediate plant biomass amounts for Day 30 (Figure 2e). This trend declined by Day 60 indicating a mixture of both terrestrial and microbial sources of DOM in the ponds with no significant differences between the fire treatments.

Fire and browning effects on DOM

DOC degradation via in situ incubation

Proportional DOC loss was more strongly linked with plant biomass than fire 10 days after plant addition (Figure 3). Proportional loss of DOC due to photodegradation was consistent across all levels of browning. Despite the nonlinear trend observed in the highest plant biomass amounts in the burned treatment, UV-only had little effect on DOC decomposition with no significant difference between fire treatments.

Microbial decomposition of DOC occurred more at intermediate plant biomass amounts with > 9 % reduction in DOC and no significant difference between fire treatments. In contrast, there was only about a 1% reduction in DOC at low and high plant biomass levels. The microbial effect on DOC degradation therefore showed a unimodal relationship with the amount of browning.

The combined effect of UV and microbes showed the greatest loss of DOC (> 13%) at intermediate biomass amounts with browning significantly impacting the rate of DOC decomposition, while fire treatment had no detectable effect.

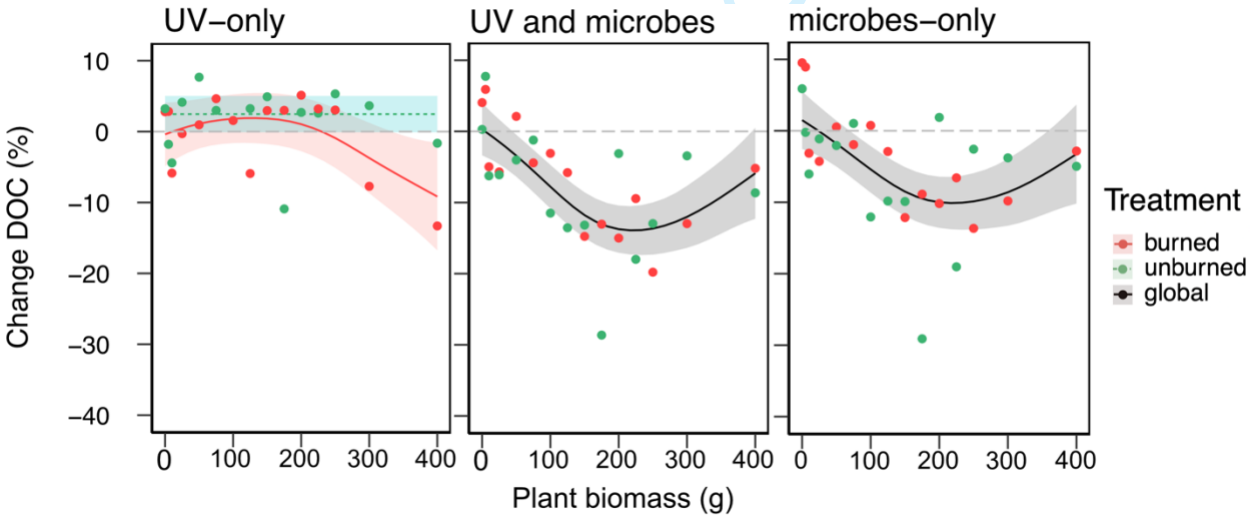

Figure 3. Dissolved organic carbon (DOC) loss as percent change for burned (red) and unburned (green) treatments across plant biomass (g). Plots with a single global smooth indicates that a model with one fit

line for the burned and unburned treatments best describes the data, while separate smooths for each fire treatment indicate that a model with different fits for the two burning treatments showed best agreement.

Dry mass decomposition of sage and willow

We calculated percent mass loss for sage and willow in relation to plant biomass and fire treatment. Sage decomposed fastest at the lowest levels of plant addition, and the relationship differed significantly between the fire treatments (p = 0.03, Figure 4a). Unburned sage exhibited a linear decrease in mass loss with increasing plant biomass whereas burned sage showed a significant nonlinear trend with the greatest mass loss at the lowest plant biomass amounts. Willow decomposition also differed significantly between the fire treatments (p = 0.02) with the most loss occurring in the unburned treatment that remained constant across plant biomass. Sage decomposed faster than willow, with the greatest difference between species in the burned treatment (p < 0.0001, Figure 4b).

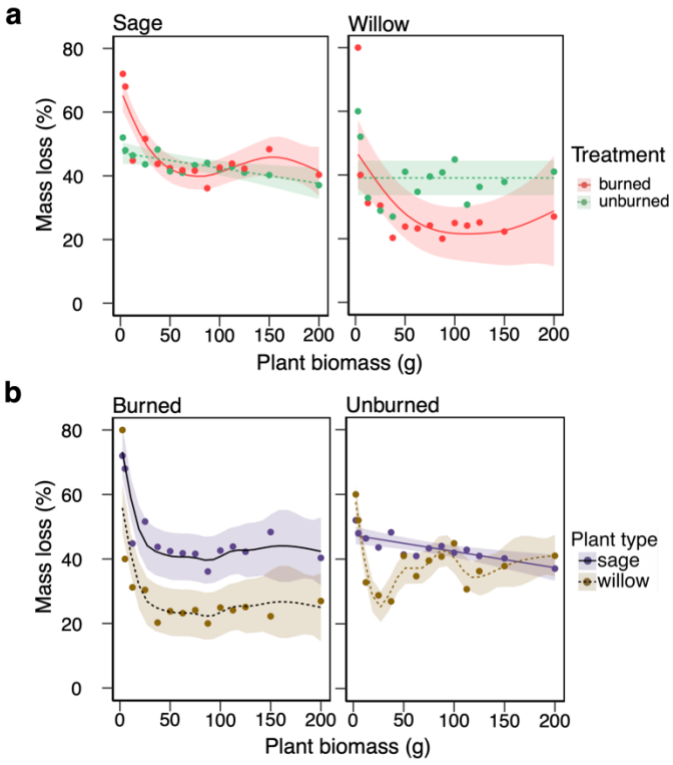

Figure 4. Percent mass loss of sage and willow across plant biomass. **a**: Mass loss for sage and willow between fire treatment. **b**: Mass loss between sage and willow within fire treatment. Plots with a single global smooth indicates that a model with one fit line for the burned and unburned treatments best describes the data, while separate smooths for each fire treatment indicate that a model with different fits for the two burning treatments showed best agreement.

Discussion

We demonstrate that loading of terrestrial plant detritus elicits nonlinear responses in the dynamics of DOM, and that DOM chemical composition is altered by fire in ways that further impact its processing and role in aquatic environments. First, we found strong nonlinear effects of plant biomass on DOC concentration, with the highest DOC concentrations early on after plant addition. DOC concentrations also differed between fire treatment which indicates that combustion from burning released stored C in the plant tissues of both willow and sage impacting the quantity of C leached as DOC into the mesocosms, especially at intermediate loading levels. The elemental chemistry of sage and willow leaves and stems in our experiment showed different responses to fire with lower C:N in severely burned tissues (C.B. Wall unpubl.). This parallels similar responses of other plant species to fire (Pellegrini et al. 2015; Wang et al. 2015; Ward et al. 2017). Based on the findings by Wang et al. (2015), and other studies cited therein, the type of burning (pyrolysis vs. thermal oxidation) and the intensity (low vs. high) are two important factors controlling C:N ratios in plant tissues that impact DOM and C cycling in aquatic systems. Furthermore, previous work has found that fire severity and DOC concentration are inversely related with lower DOC concentrations associated with high-severity fires (Santos et al. 2019). The fire severity at which the plant material was

burned in our study could explain the nonlinear patterns in DOC concentration given that the burned plant material experienced only one regime (likely high severity pyrolysis).

The differences in DOC concentration between fire treatments became less over time, and more linear across the biomass gradient. The role of residence time as it relates to DOC from burned or unburned detritus could be another major factor controlling DOM cycling in aquatic systems insofar that detrital loading exceeds the rate of DOM turnover (Stedmon and Nelson 2015); future studies using a similar experimental design should not only measure DOM change over longer periods to better understand the potential physio-chemical effects of fire and residence time on the DOM pool but also incorporate other factors like total lake area or temperature that contribute to DOC concentration variability (e.g., Hanson et al. 2011). Our gradient design demonstrates a general nonlinear pattern associated with increasing plant detritus which may be typical for the fate of DOM in aquatic ecosystems that experience loading from severely burned watersheds.

Second, the different shapes of the functions relating DOC concentration to terrestrial loading rather than changes to DOM chemistry from fire explain the patterns observed among the in situ incubations. DOC decomposition was more strongly linked to the rate of browning than fire as evidenced by the unimodal shape of the proportional rate of decomposition as a function of plant biomass (Figure 3). For instance, there was greater DOC loss by biodegradation compared to photodegradation at intermediate loading levels. Previous studies using first-order decay models of microbial decomposition of DOC (Wilske et al. 2020; Chen et al. 2022) found that the rate of loss is proportional to initial concentrations, a likely explanation for why we saw less change in DOC at the lowest plant biomass amounts; while at the highest biomass amounts,

hypoxia caused by biological demand (Figure S8), inhibited microbial respiration and caused DOC to persist in the water rather than be degraded.

The compositional shifts indicated by the fluorescence and UV-vis absorbance indices further suggest that the effects of microbes in response to browning on DOC decomposition is stronger than photodegradation. For example, the higher FI values and the greater intensities of B and M peaks (Figure S4) seen early on after plant addition have been found to be associated with bacterial biomass and represent products of bacterial metabolism also found in lakes (Determann et al. 1998; Cammack et al. 2004). Moreover, previous work has shown that aromatic, humic compounds can moderate bacterial activity through photochemical transformations that yield labile compounds (i.e., a primary bacterial substrate) (Moran and Hodson 1990; Cory and Kling 2018). While our primary focus was on whether photo- or biodegradation contributed more to DOC loss along a gradient of increasing plant biomass, a successive photochemical-microbial degradation pathway (i.e., UV and microbes) contributed to the greatest DOC loss at these intermediate biomass levels. Further study should focus on the rate of degradation and molecular change over a continuous temporal scale to disentangle the interactive effects of photo- and microbial processes. The patterns in the concentrations of biologically and photochemically degradable DOC reported here show the importance of identifying DOM compounds and environmental factors linked to fire-affected aquatic systems.

It is important to note that this study differs from previous work on microbial decomposition of DOM since our filtering likely reduced the abundance of microbes in the incubation experiment but did not completely exclude them. The GF/F pore size used (0.7 μm) allowed the passage of some microorganisms. While the disinfecting quality of exposure to UV radiation may have reduced bacterial abundance in the photodegradation experiment (Yang et al.

2020; Uzun et al. 2020), filtering reduced DOC decomposition across most plant biomass amounts, suggesting that removing microorganisms, even if incomplete, impedes decomposition.

Third, fire altered some of the chemical properties of DOM and influenced the rate of particulate organic matter processing. The spectroscopic (UV-vis absorbance and fluorescence) indices show reduced humification in the burned treatment, but greater aromaticity in both fire treatments with time. Chemical fractionation driven by high severity pyrolysis (see Wang et al. 2015) likely explains the compositional differences between the burned and unburned treatments for HIX, specifically. The differences in chemical fractionation of humified DOM indicates that burning produces hydrophobic DOM rather than hydrophilic DOM, resulting in lower solubility of high MW, aromatic structures that are less susceptible to processing (Wang et al. 2015). This reduced processing manifested as lower HIX values in the burned treatment over time, a finding also supported in the EEMs with lower terrestrial humic-like DOM (regions A and C in Figure S4-S7). DOM from burned and unburned sources is processed but at varying rates leading to the differences in humification over time; the processing of DOM in the mesocosms can be further supported by the trends in $SUVA_{254}$ which indicate that labile compounds were degraded early on after plant addition leading to the accumulation of recalcitrant DOM over time. The interaction between browning and fire alters the rate at which DOM is processed with distinct differences in the humification between burned and unburned detrital sources and the overall accumulation of aromatic compounds in the system, demonstrating how wildfire can be an important controlling factor on C cycling in freshwater systems.

Finally, we found clear influences of fire treatment and browning on the decomposition of willow and sage suggesting that fire impacts the processing of particulate organic detritus in aquatic systems. Previous studies have shown that woody structures decompose more slowly

than leaves (Cornelissen et al. 2017). The detritus in our experiment included woody and leafy parts of both plant species. However, fire can affect plant material by either reducing its availability as a substrate for microbial decomposition, or altering its chemical structure (e.g., by charring or limited oxygen availability) which decreases its decomposability (Bostick et al. 2021). The fact that willow decomposed less than sage in our study suggests an effect of its specific physiology such as its lignin-rich tissues or woody structure. Therefore, the traits of different plant species may greatly influence their rates of decomposition. Plant community composition is important for fire regimes because the functional traits of different species impose strong effects on litter quality (Cornwell et al. 2009). As browning and wildfire are projected to increase (Bowman et al. 2009; Kritzberg et al. 2020) future work should consider the heterogeneity of the surrounding vegetation near a watershed with a framework that includes a greater variety of plant species. Our experiment reveals that the loading of terrestrially derived detritus alters the shape of the nonlinear functions relating to DOM chemistry and fire treatment, and that both fire and browning jointly impact the fate of DOM in the aquatic mesocosms.

Conclusions and Implications

Browning and transformations due to fire affect the chemistry of DOM in surface waters and therefore its rate of degradation due to microbial respiration. The concentration and chemical composition of DOM along a gradient of increasing plant detrital loading provided evidence for greater microbial degradation as seen in the compositional shifts in the EEMs, trends in the fluorescence and UV-vis absorbance indices, and the incubation experiment. These results are important because many studies have shown that the ability of microorganisms to uptake and respire DOM depends on its initial chemistry (Cory et al. 2007; Cory and Kling 2018; Berggren

et al. 2022). Therefore, our results imply that the browning of lakes may increase microbial mineralization of DOC at low to intermediate concentrations but impede it at higher levels when biological demand depletes dissolved oxygen concentrations. These changes in the conditions that affect microbial activity can in turn affect carbon processing (e.g., storage in sediments vs. mineralization as CO_2) and export to the ocean. Nonlinear changes to the structure and function of aquatic ecosystems affects their capacity to store and process DOC, and their role in the global C cycle.

References

Abatzoglou, J. T., and A. P. Williams. 2016. Impact of anthropogenic climate change on wildfire across western US forests. 6.

Allen, E. W., E. E. Prepas, S. Gabos, W. Strachan, and W. Chen. 2003. Surface water chemistry of burned and undisturbed watersheds on the Boreal Plain: an ecoregion approach. **2**: 14.

Berggren, M., F. Guillemette, M. Bieroza, and others. 2022. Unified understanding of intrinsic and extrinsic controls of dissolved organic carbon reactivity in aquatic ecosystems. 41.

Bertilsson, S., and L. J. Tranvik. 2000. Photochemical transformation of dissolved organic matter in lakes. Limnol. Oceanogr. **45**: 753–762. doi:10.4319/lo.2000.45.4.0753

Bond, W. 2013. Fires, Ecological Effects of. Encycl. Biodivers. **3**: 435–442. doi:10.1016/B978-0-12-384719-5.00053-8

Bostick, K. W., A. R. Zimmerman, A. I. Goranov, S. Mitra, P. G. Hatcher, and A. S. Wozniak. 2021. Biolability of Fresh and Photodegraded Pyrogenic Dissolved Organic Matter From Laboratory-Prepared Chars. J. Geophys. Res. Biogeosciences **126**. doi:10.1029/2020JG005981

Bowman, D. M. J. S., J. K. Balch, P. Artaxo, and others. 2009. Fire in the Earth System. Science **324**: 481–484. doi:10.1126/science.1163886

Bowring, S. P. K., M. W. Jones, P. Ciais, B. Guenet, and S. Abiven. 2022. Pyrogenic carbon decomposition critical to resolving fire's role in the Earth system. Nat. Geosci. **15**: 135–142. doi:10.1038/s41561-021-00892-0

Burton, C., D. I. Kelley, C. D. Jones, R. A. Betts, M. Cardoso, and L. Anderson. 2022. South American fires and their impacts on ecosystems increase with continued emissions. Clim. Resil. Sustain. **1**. doi:10.1002/cli2.8

545 Cammack, W. K. L., J. Kalff, Y. T. Prairie, and E. M. Smith. 2004. Fluorescent dissolved
546 organic matter in lakes: Relationships with heterotrophicmetabolism. Limnol. Oceanogr.
547 **49**: 2034–2045. doi:10.4319/lo.2004.49.6.2034
548 Campos, I., and N. Abrantes. 2021. Forest fires as drivers of contamination of polycyclic
549 aromatic hydrocarbons to the terrestrial and aquatic ecosystems. Curr. Opin. Environ. Sci.
550 Health **24**: 100293. doi:10.1016/j.coesh.2021.100293
551 Chen, Y., K. Sun, H. Sun, Y. Yang, Y. Li, B. Gao, and B. Xing. 2022. Photodegradation of
552 pyrogenic dissolved organic matter increases bioavailability: Novel insight into
553 bioalteration, microbial community succession, and C and N dynamics. Chem. Geol. **605**:
554 1–14. doi:10.1016/j.chemgeo.2022.120964
555 Coble, P. G. 1996. Characterization of marine and terrestrial DOM in seawater using excitation-
556 emission matrix spectroscopy. Mar. Chem. **51**: 325–346. doi:10.1016/0304-
557 4203(95)00062-3
558 Coble, P. G. 2007. Marine Optical Biogeochemistry: The Chemistry of Ocean Color. Chem. Rev.
559 **107**: 402–418. doi:10.1021/cr050350+
560 Cole, J. J., Y. T. Prairie, N. F. Caraco, and others. 2007. Plumbing the Global Carbon Cycle:
561 Integrating Inland Waters into the Terrestrial Carbon Budget. Ecosystems **10**: 172–185.
562 doi:10.1007/s10021-006-9013-8
563 Cooper, S. D., H. M. Page, S. W. Wiseman, and others. 2015. Physicochemical and biological
564 responses of streams to wildfire severity in riparian zones. Freshw. Biol. **60**: 2600–2619.
565 doi:10.1111/fwb.12523

566 Cornelissen, J. H. C., S. Grootemaat, L. M. Verheijen, W. K. Cornwell, P. M. Bodegom, R. Wal,
567 and R. Aerts. 2017. Are litter decomposition and fire linked through plant species traits?
568 New Phytol. **216**: 653–669. doi:10.1111/nph.14766
569 Cornwell, W. K., J. H. C. Cornelissen, S. D. Allison, and others. 2009. Plant traits and wood
570 fates across the globe: rotted, burned, or consumed? Glob. Change Biol. **15**: 2431–2449.
571 doi:10.1111/j.1365-2486.2009.01916.x
572 Cory, R. M., and G. W. Kling. 2018. Interactions between sunlight and microorganisms
573 influence dissolved organic matter degradation along the aquatic continuum. Limnol.
574 Oceanogr. Lett. **3**: 102–116. doi:10.1002/lol2.10060
575 Cory, R. M., D. M. McKnight, Y.-P. Chin, P. Miller, and C. L. Jaros. 2007. Chemical
576 characteristics of fulvic acids from Arctic surface waters: Microbial contributions and
577 photochemical transformations: CHARACTERISTICS OF ARCTIC FULVIC ACIDS. J.
578 Geophys. Res. Biogeosciences **112**: n/a-n/a. doi:10.1029/2006JG000343
579 D'Antonio, C. M., and P. M. Vitousek. 1992. Biological Invasions by Exotic Grasses, the
580 Grass/Fire Cycle, and Global Change. Annu. Rev. Ecol. Evol. Syst. 23–63.
581 Dempsey, C. M., J. A. Brentrup, S. Magyan, and others. 2020. The relative importance of
582 photodegradation and biodegradation of terrestrially derived dissolved organic carbon
583 across four lakes of differing trophic status. Biogeosciences **17**: 6327–6340.
584 doi:10.5194/bg-17-6327-2020
585 Denis, M., L. Jeanneau, A.-C. Pierson-Wickman, G. Humbert, P. Petitjean, A. Jaffrézic, and G.
586 Gruau. 2017. A comparative study on the pore-size and filter type effect on the molecular
587 composition of soil and stream dissolved organic matter. Org. Geochem. **110**: 36–44.
588 doi:10.1016/j.orggeochem.2017.05.002

589 Determann, S., J. M. Lobbes, R. Reuter, and J. Rullkötter. 1998. Ultraviolet fluorescence
590 excitation and emission spectroscopy of marine algae and bacteria. Mar. Chem. **62**: 137–
591 156. doi:10.1016/S0304-4203(98)00026-7
592 Earl, S. R., and D. W. Blinn. 2003. Effects of wildfire ash on water chemistry and biota in South-
593 Western U.S.A. streams. Freshw. Biol. 16.
594 Fonseca, B. M., E. E. Levi, L. W. Jensen, D. Graeber, M. Søndergaard, T. L. Lauridsen, E.
595 Jeppesen, and T. A. Davidson. 2022. Effects of DOC addition from different sources on
596 phytoplankton community in a temperate eutrophic lake: An experimental study
597 exploring lake compartments. Sci. Total Environ. **803**: 150049.
598 doi:10.1016/j.scitotenv.2021.150049
599 Granath, G., C. D. Evans, J. Strengbom, J. Fölster, A. Grelle, J. Strömqvist, and S. J. Köhler.
600 2021. The impact of wildfire on biogeochemical fluxes and water quality in boreal
601 catchments. Biogeosciences **18**: 3243–3261. doi:10.5194/bg-18-3243-2021
602 Halofsky, J. E., D. L. Peterson, and B. J. Harvey. 2020. Changing wildfire, changing forests: the
603 effects of climate change on fire regimes and vegetation in the Pacific Northwest, USA.
604 Fire Ecol. **16**: 4. doi:10.1186/s42408-019-0062-8
605 Hanson, P. C., D. L. Bade, S. R. Carpenter, and T. K. Kratz. 2003. Lake metabolism:
606 Relationships with dissolved organic carbon and phosphorus. Limnol. Oceanogr. **48**:
607 1112–1119. doi:10.4319/lo.2003.48.3.1112
608 Hanson, P. C., D. P. Hamilton, E. H. Stanley, N. Preston, O. C. Langman, and E. L. Kara. 2011.
609 Fate of Allochthonous Dissolved Organic Carbon in Lakes: A Quantitative Approach T.
610 Evens [ed.]. PLoS ONE **6**: e21884. doi:10.1371/journal.pone.0021884

611 Harvey, B. J., and N. J. Enright. 2022. Climate change and altered fire regimes: impacts on plant
612 populations, species, and ecosystems in both hemispheres. Plant Ecol. s11258-022-
613 01248–3. doi:10.1007/s11258-022-01248-3
614 Helms, J. R., A. Stubbins, E. M. Perdue, N. W. Green, H. Chen, and K. Mopper. 2013.
615 Photochemical bleaching of oceanic dissolved organic matter and its effect on absorption
616 spectral slope and fluorescence. Mar. Chem. **155**: 81–91.
617 doi:10.1016/j.marchem.2013.05.015
618 Helms, J. R., A. Stubbins, J. D. Ritchie, E. C. Minor, D. J. Kieber, and K. Mopper. 2008.
619 Absorption spectral slopes and slope ratios as indicators of molecular weight, source, and
620 photobleaching of chromophoric dissolved organic matter. Limnol. Oceanogr. **53**: 955–
621 969. doi:10.4319/lo.2008.53.3.0955
622 Keeley, J. E., and C. J. Fotheringham. 2001. Historic Fire Regime in Southern California
623 Shrublands. Conserv. Biol. **15**: 1536–1548. doi:10.1046/j.1523-1739.2001.00097.x
624 Khan, E., and S. Subramania-Pillai. 2006. Effect of Leaching from Filters on Laboratory
625 Analyses of Collective Organic Constituents. Proc. Water Environ. Fed. **2006**: 901–918.
626 doi:10.2175/193864706783749747
627 Kritzberg, E. S., E. M. Hasselquist, M. Škerlep, and others. 2020. Browning of freshwaters:
628 Consequences to ecosystem services, underlying drivers, and potential mitigation
629 measures. Ambio **49**: 375–390. doi:10.1007/s13280-019-01227-5
630 Larsen, I. J., L. H. MacDonald, E. Brown, and others. 2009. Causes of Post-Fire Runoff and
631 Erosion: Water Repellency, Cover, or Soil Sealing? Soil Sci. Soc. Am. J. **73**: 1393–1407.
632 doi:10.2136/sssaj2007.0432

633 Lasslop, G., A. I. Coppola, A. Voulgarakis, C. Yue, and S. Veraverbeke. 2019. Influence of Fire
634 on the Carbon Cycle and Climate. Curr. Clim. Change Rep. **5**: 112–123.
635 doi:10.1007/s40641-019-00128-9
636 Laurion, I., and N. Mladenov. 2013. Dissolved organic matter photolysis in Canadian arctic thaw
637 ponds. Env. Res Lett 13.
638 Lavabre, J., D. S. Torres, and F. Cernesson. 1993. Changes in the hydrological response of a
639 small Mediterranean basin a year after a wildfire. J. Hydrol. **142**: 273–299.
640 doi:10.1016/0022-1694(93)90014-Z
641 Lewis, J., J. J. Rhodes, and C. Bradley. 2019. Turbidity Responses from Timber Harvesting,
642 Wildfire, and Post-Fire Logging in the Battle Creek Watershed, Northern California.
643 Environ. Manage. **63**: 416–432. doi:10.1007/s00267-018-1036-3
644 Magyan, S., and C. M. Dempsey. 2021. The role of time and mixing in the degradation of
645 terrestrial derived dissolved organic carbon in lakes of varying trophic status. J.
646 Photochem. Photobiol. **8**: 1–7. doi:10.1016/j.jpap.2021.100065
647 McCullough, I. M., K. S. Cheruvelil, J. Lapierre, N. R. Lottig, M. A. Moritz, J. Stachelek, and P.
648 A. Soranno. 2019. Do lakes feel the burn? Ecological consequences of increasing
649 exposure of lakes to fire in the continental United States. Glob. Change Biol. **25**: 2841–
650 2854. doi:10.1111/gcb.14732
651 McEachern, P., E. E. Prepas, J. J. Gibson, and W. P. Dinsmore. 2000. Forest fire induced
652 impacts on phosphorus, nitrogen, and chlorophyll a concentrations in boreal subarctic
653 lakes of northern Alberta. **57**: 9.
654 McKenzie, D., Z. Gedalof, D. L. Peterson, and P. Mote. 2004. Climatic Change, Wildfire, and
655 Conservation. Conserv. Biol. **18**: 890–902. doi:10.1111/j.1523-1739.2004.00492.x

McKnight, D. M., E. W. Boyer, P. K. Westerhoff, P. T. Doran, T. Kulbe, and D. T. Andersen. 2001. Spectrofluorometric characterization of dissolved organic matter for indication of precursor organic material and aromaticity. Limnol. Oceanogr. **46**: 38–48. doi:10.4319/lo.2001.46.1.0038

Moody, J. A., and D. A. Martin. 2001. Initial hydrologic and geomorphic response following a wildfire in the Colorado Front Range. Earth Surf. Process. Landf. **26**: 1049–1070. doi:10.1002/esp.253

Moran, M. A., and R. E. Hodson. 1990. Bacterial production on humic and nonhumic components of dissolved organic carbon. Limnol. Oceanogr. **35**: 1744–1756. doi:10.4319/lo.1990.35.8.1744

Morris, D. P., and B. R. Hargreaves. 1997. The role of photochemical degradation of dissolved organic carbon in regulating the UV transparency of three lakes on the Pocono Plateau. Limnol. Oceanogr. **42**: 239–249. doi:10.4319/lo.1997.42.2.0239

Mulholland, P. J., and J. W. Elwood. 1982. The role of lake and reservoir sediments as sinks in the perturbed global carbon cycle. Tellus **34**: 490–499. doi:10.1111/j.2153-3490.1982.tb01837.x

Obernosterer, I., and R. Benner. 2004. Competition between biological and photochemical processes in the mineralization of dissolved organic carbon. Limnol. Oceanogr. **49**: 117–124. doi:10.4319/lo.2004.49.1.0117

Parlanti, E. 2000. Dissolved organic matter ¯uorescence spectroscopy as a tool to estimate biological activity in a coastal zone submitted to anthropogenic inputs. Org. Geochem. **31**.

678 Pellegrini, A. F. A., L. O. Hedin, A. C. Staver, and N. Govender. 2015. Fire Alters Ecosystem
679 Carbon and Nutrients but not Plant Nutrient Stoichiometry. Bull. Ecol. Soc. Am. **96**:
680 340–343. doi:10.1890/0012-9623-96.2.340
681 Pereira, P., X. Úbeda, D. Martin, J. Mataix-Solera, and C. Guerrero. 2011. Effects of a low
682 severity prescribed fire on water-soluble elements in ash from a cork oak (Quercus suber)
683 forest located in the northeast of the Iberian Peninsula. Environ. Res. **111**: 237–247.
684 doi:10.1016/j.envres.2010.09.002
685 Santos, F., A. S. Wymore, B. K. Jackson, S. M. P. Sullivan, W. H. McDowell, and A. A. Berhe.
686 2019. Fire severity, time since fire, and site-level characteristics influence streamwater
687 chemistry at baseflow conditions in catchments of the Sierra Nevada, California, USA.
688 Fire Ecol. **15**: 3. doi:10.1186/s42408-018-0022-8
689 Stedmon, C. A., and N. B. Nelson. 2015. The Optical Properties of DOM in the Ocean, p. 481–
690 508. *In* Biogeochemistry of Marine Dissolved Organic Matter. Elsevier.
691 Stevens-Rumann, C., and P. Morgan. 2016. Repeated wildfires alter forest recovery of mixed-
692 conifer ecosystems. Ecol. Appl. **26**: 1842–1853. doi:10.1890/15-1521.1
693 Uzun, H., R. A. Dahlgren, C. Olivares, C. U. Erdem, T. Karanfil, and A. T. Chow. 2020. Two
694 years of post-wildfire impacts on dissolved organic matter, nitrogen, and precursors of
695 disinfection by-products in California stream waters. Water Res. **181**: 115891.
696 doi:10.1016/j.watres.2020.115891
697 Wagner, S., R. Jaffé, and A. Stubbins. 2018. Dissolved black carbon in aquatic ecosystems.
698 Limnol. Oceanogr. Lett. **3**: 168–185. doi:10.1002/lol2.10076
699 Wang, J.-J., R. A. Dahlgren, and A. T. Chow. 2015. Controlled Burning of Forest Detritus
700 Altering Spectroscopic Characteristics and Chlorine Reactivity of Dissolved Organic

Matter: Effects of Temperature and Oxygen Availability. Environ. Sci. Technol. **49**: 14019–14027. doi:10.1021/acs.est.5b03961

Ward, N. D., T. S. Bianchi, P. M. Medeiros, M. Seidel, J. E. Richey, R. G. Keil, and H. O. Sawakuchi. 2017. Where Carbon Goes When Water Flows: Carbon Cycling across the Aquatic Continuum. Front. Mar. Sci. **4**. doi:10.3389/fmars.2017.00007

Weishaar, J. L., G. R. Aiken, B. A. Bergamaschi, M. S. Fram, R. Fujii, and K. Mopper. 2003. Evaluation of Specific Ultraviolet Absorbance as an Indicator of the Chemical Composition and Reactivity of Dissolved Organic Carbon. Environ. Sci. Technol. **37**: 4702–4708. doi:10.1021/es030360x

Wetzel, R. G. 1984. Detrital Dissolved and Particulate Organic Carbon Functions in Aquatic Ecosystems. Bull. Mar. Sci. **35**: 503–509.

Wilske, C., P. Herzsprung, O. J. Lechtenfeld, N. Kamjunke, and W. von Tümpling. 2020a. Photochemically Induced Changes of Dissolved Organic Matter in a Humic-Rich and Forested Stream. Water **12**: 331. doi:10.3390/w12020331

Wilske, C., P. Herzsprung, O. J. Lechtenfeld, N. Kamjunke, and W. von Tümpling. 2020b. Photochemically Induced Changes of Dissolved Organic Matter in a Humic-Rich and Forested Stream. Water **12**: 331. doi:10.3390/w12020331

Wood, S. N. 2017. Generalized Additive Models: An Introduction with R, Second Edition, 2nd Edition. Chapman and Hall/CRC.

Yang, C., W. Sun, and X. Ao. 2020. Bacterial inactivation, DNA damage, and faster ATP degradation induced by ultraviolet disinfection. Front. Environ. Sci. Eng. **14**: 13. doi:10.1007/s11783-019-1192-6

723 Zedler, P. H., C. R. Gautier, and G. S. McMaster. 1983. Vegetation Change in Response to
724 Extreme Events: The Effect of a Short Interval between Fires in California Chaparral and
725 Coastal Scrub. Ecology **64**: 809–818. doi:10.2307/1937204
726 Zsolnay, A., E. Baigar, M. Jimenez, B. Steinweg, and F. Saccomandi. 1999. Differentiating with
727 fluorescence spectroscopy the sources of dissolved organic matter in soils subjected to
728 drying. Chemosphere **38**: 45–50. doi:10.1016/S0045-6535(98)00166-0

729

730 **Acknowledgements:**
731 We thank Keyshawn Ford, Bautista Tobias, Kirby Inocente, Tristie Le, and Ariana Brisco-
732 Schoefield for their assistance, and Dr. Eric Schmelz for logistical support. This project was
733 funded by support from NSF DEB 2018058.

734

735 **Data accessibility**
736 All data and scripts are available at Github (http://www.github.com/cjspiegs/Pyromania) and are
737 archived at Zenodo (xxx – will update following peer review).

738

739

740

741

742

743

744

745

Supplemental Tables

Table S1. Model selection for dissolved organic carbon (DOC) concentration candidate GAM models* assessed with Akaike Information Criterion (AIC) at Days-10, 31, 59, and 89.

Variable	Model	df	AIC
DOC concentration	Day 10: Treatment with by–factor smooth	10.859	**147**
	Day 10: Treatment with global smooth	6.597	158
	Day 10: global smooth	5.480	162
	Day 31: Treatment with by–factor smooth	12.461	**118**
	Day 31: Treatment with global smooth	6.269	160
	Day 31: global smooth	5.333	158
	Day 59: Treatment with by–factor smooth	8.245	**64**
	Day 59: Treatment with global smooth	4.000	70
	Day 59: global smooth	3.000	76
	Day 89: Treatment with by–factor smooth	6.324	111
	Day 89: Treatment with global smooth	5.389	109
	Day 89: global smooth	4.384	**108**

**Treatment with by-factor smooth* has parametric terms (*Treatment*) and separate smooths for each fire treatment; *Treatment with global smooth* uses an estimated mean allowing for off-set intercepts according to fire treatment. The *global smooth* fits one estimated mean as a global smooth to all data. *Bolded* lowest AIC values represent the selected models.

Fire and browning effects on DOM

Table S2. Model selection for fluorescence and UV-vis absorbance indices with candidate GAM models* assessed with Akaike Information Criterion (AIC) at Days-10, 31, 59, and 89.

Variable	Model	df	AIC
SUVA	Day 10: Treatment with by–factor smooth	11.829	**16**
	Day 10: Treatment with global smooth	7.758	18
	Day 10: global smooth	6.762	17
	Day 31: Treatment with by–factor smooth	6.560	**166**
	Day 31: Treatment with global smooth	5.095	168
	Day 31: global smooth	4.087	167
	Day 59: Treatment with by–factor smooth	10.018	**23**
	Day 59: Treatment with global smooth	7.067	28
	Day 59: global smooth	5.518	36
	Day 89: Treatment with by–factor smooth	6.949	**33**
	Day 89: Treatment with global smooth	5.560	38
	Day 89: global smooth	4.576	36
HIX	Day 10: Treatment with by–factor smooth	5.000	62
	Day 10: Treatment with global smooth	4.000	60
	Day 10: global smooth	3.000	**59**
	Day 31: Treatment with by–factor smooth	5.000	30
	Day 31: Treatment with global smooth	4.000	**28**
	Day 31: global smooth	3.000	28
	Day 59: Treatment with by–factor smooth	11.953	**23**
	Day 59: Treatment with global smooth	7.757	24
	Day 59: global smooth	5.936	35
	Day 89: Treatment with by–factor smooth	10.053	**25**
	Day 89: Treatment with global smooth	6.208	41
	Day 89: global smooth	4.841	52
Slope ratio	Day 10: Treatment with by–factor smooth	7.127	**7**
	Day 10: Treatment with global smooth	5.172	12
	Day 10: global smooth	4.186	11
	Day 31: Treatment with by–factor smooth	11.537	–13
	Day 31: Treatment with global smooth	7.677	–20
	Day 31: global smooth	6.712	**–22**
	Day 59: Treatment with by–factor smooth	9.688	–1
	Day 59: Treatment with global smooth	6.776	**–7**
	Day 59: global smooth	5.747	–6
	Day 89: Treatment with by–factor smooth	11.398	**–57**
	Day 89: Treatment with global smooth	7.363	–42
	Day 89: global smooth	6.396	–44
FR	Day 10: Treatment with by–factor smooth	6.194	**–5**
	Day 10: Treatment with global smooth	4.000	0
	Day 10: global smooth	3.000	2
	Day 31: Treatment with by–factor smooth	6.756	**–102**
	Day 31: Treatment with global smooth	5.460	–101
	Day 31: global smooth	4.296	–96
	Day 59: Treatment with by–factor smooth	8.337	–104
	Day 59: Treatment with global smooth	6.186	**–108**
	Day 59: global smooth	4.617	–86
	Day 89: Treatment with by–factor smooth	9.278	–103
	Day 89: Treatment with global smooth	7.825	**–104**
	Day 89: global smooth	3.470	–93
FI	Day 10: Treatment with by–factor smooth	6.893	**40**
	Day 10: Treatment with global smooth	5.277	43
	Day 10: global smooth	4.300	42
	Day 31: Treatment with by–factor smooth	10.411	**–55**
	Day 31: Treatment with global smooth	5.358	–45
	Day 31: global smooth	4.351	–46
	Day 59: Treatment with by–factor smooth	7.129	–46
	Day 59: Treatment with global smooth	5.565	–48
	Day 59: global smooth	4.546	**–49**
	Day 89: Treatment with by–factor smooth	6.425	–21
	Day 89: Treatment with global smooth	4.000	–23
	Day 89: global smooth	3.000	**–24**

766 **Treatment with by-factor smooth* has parametric terms (*Treatment*) and separate smooths for each fire treatment;
767 *Treatment with global smooth* uses an estimated mean allowing for off-set intercepts according to fire treatment. The
768 *global smooth* fits one estimated mean as a global smooth to all data. *Bolded* lowest AIC values represent the
769 selected models.
770
771
772
773
774
775
776
777
778
779
780
781
782
783
784
785
786
787
788
789

Fire and browning effects on DOM

790 **Table S3**. Model selection for percent DOC change with candidate GAM models* assessed in
791 each incubation condition (UV-only, Microbes-only, UV and microbes) with Akaike Information
792 Criterion (AIC) at Days-10, 31, 59, and 89.

Variable	Model	df	AIC
Plant mass	UV–only: Treatment with by–factor smooth	3.000	198
	UV–only: Treatment with global smooth	3.000	198
	UV–only: global smooth	2.000	**197**
	Microbes–only: Treatment with by–factor smooth	9.594	186
	Microbes–only: Treatment with global smooth	6.703	182
	Microbes–only: global smooth	5.692	**181**
	UV and microbes: Treatment with by–factor smooth	9.659	186
	UV and microbes: Treatment with global smooth	6.971	181
	UV and microbes: global smooth	6.013	**179**
SUVA	UV–only: Treatment with by–factor smooth	3.000	198
	UV–only: Treatment with global smooth	3.000	198
	UV–only: global smooth	2.000	**197**
	Microbes–only: Treatment with by–factor smooth	7.608	193
	Microbes–only: Treatment with global smooth	5.845	192
	Microbes–only: global smooth	4.862	**191**
	UV and microbes: Treatment with by–factor smooth	7.608	193
	UV and microbes: Treatment with global smooth	5.741	190
	UV and microbes: global smooth	4.792	**188**
HIX	UV–only: Treatment with by–factor smooth	6.958	183
	UV–only: Treatment with global smooth	7.343	**182**
	UV–only: global smooth	5.743	190
	Microbes–only: Treatment with by–factor smooth	5.200	208
	Microbes–only: Treatment with global smooth	8.010	198
	Microbes–only: global smooth	7.085	**197**
	UV and microbes: Treatment with by–factor smooth	5.142	211
	UV and microbes: Treatment with global smooth	8.532	200
	UV and microbes: global smooth	7.661	**198**

793

794 **Treatment with by-factor smooth* has parametric terms (*Treatment*) and separate smooths for each fire treatment;
795 *Treatment with global smooth* uses an estimated mean allowing for off-set intercepts according to fire treatment. The
796 *global smooth* fits one estimated mean as a global smooth to all data. *Bolded* lowest AIC values represent the
797 selected models.

Fire and browning effects on DOM

Table S4. Model selection for percent mass loss with candidate GAM models* assessed with Akaike Information Criterion (AIC) at Days-10, 31, 59, and 89 for each plant type (sage and willow) by fire treatment.

Variable	Model	df	AIC
Plant mass	Sage: Treatment with by–factor smooth	9.047	**167**
	Sage: Treatment with global smooth	6.518	181
	Sage: global smooth	5.350	183
	Willow: Treatment with by–factor smooth	5.781	**217**
	Willow: Treatment with global smooth	3.000	251
	Willow: global smooth	4.399	223
	Burned: plant type with by–factor smooth	10.253	206
	Burned: plant type with global smooth	9.239	200
	Burned: global smooth	5.112	226
	Unburned: plant type with by–factor smooth	11.762	**155**
	Unburned: plant type with global smooth	8.544	181
	Unburned: global smooth	7.007	185

**Treatment with by-factor smooth* has parametric terms (*Treatment*) and separate smooths for each fire treatment; *Treatment with global smooth* uses an estimated mean allowing for off-set intercepts according to fire treatment. The *global smooth* fits one estimated mean as a global smooth to all data. *Bolded* lowest AIC values represent the selected models.

Supplemental Figures

Figure S1. Pictures of the two severity groups taken after burning **a:** low severity and **b:** high severity.

Fire and browning effects on DOM

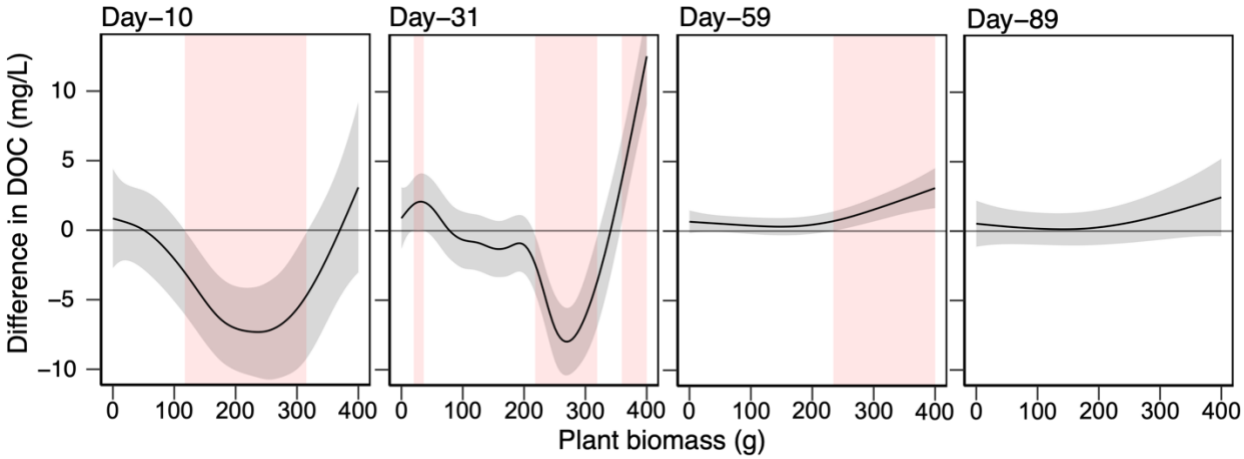

Figure S2. Differences in dissolved organic carbon (DOC) concentration for fitted smooth functions between fire treatments (burned vs. unburned) across plant biomass. Difference in trends shown in red with approximate 95% confidence intervals.

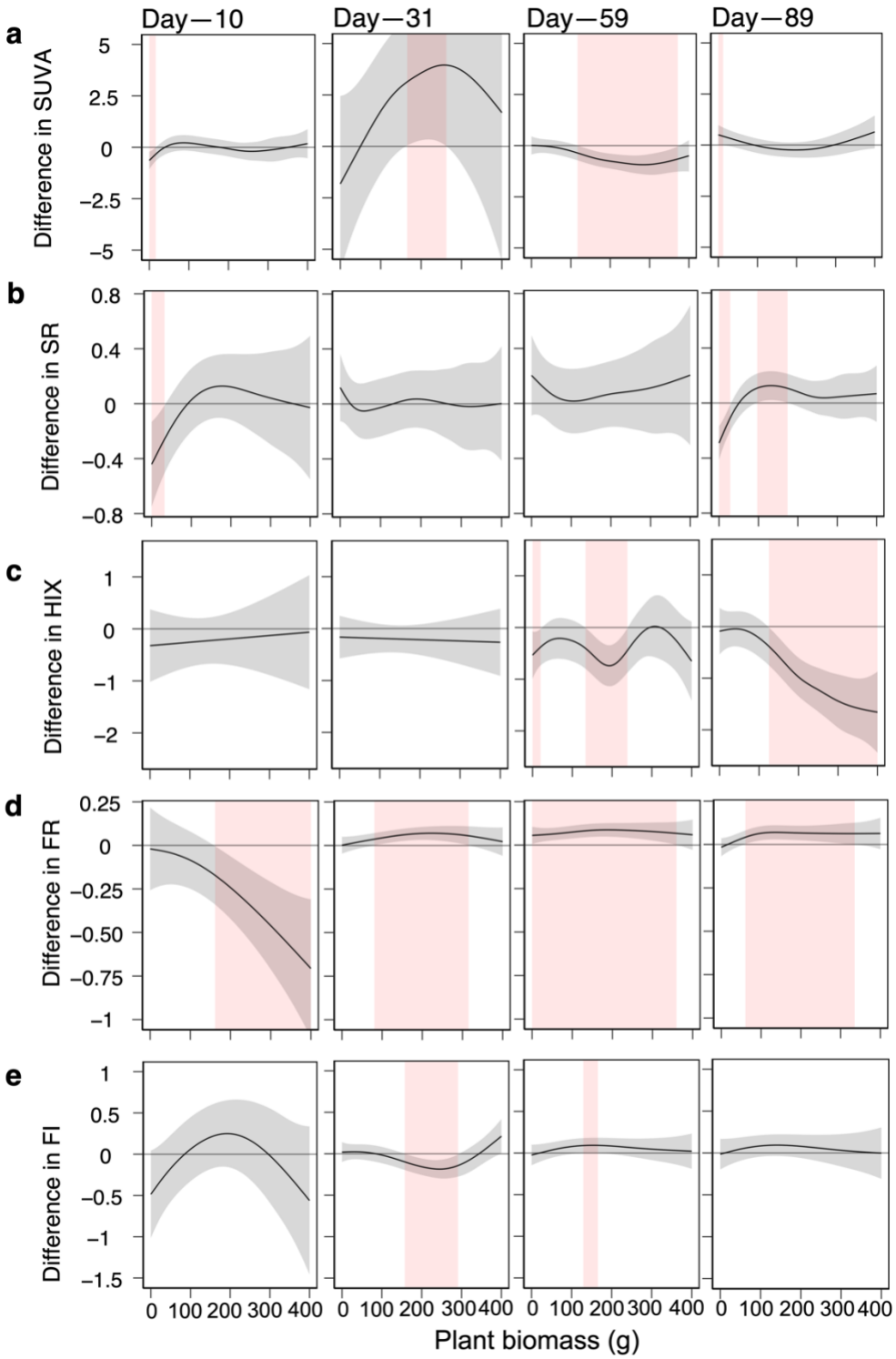

Figure S3. Differences between fitted smooth functions between the fire treatments (difference in trends; solid lines) for fluorescence and UV-vis absorbance indices shown in red with approximate 95% confidence intervals.

Fire and browning effects on DOM

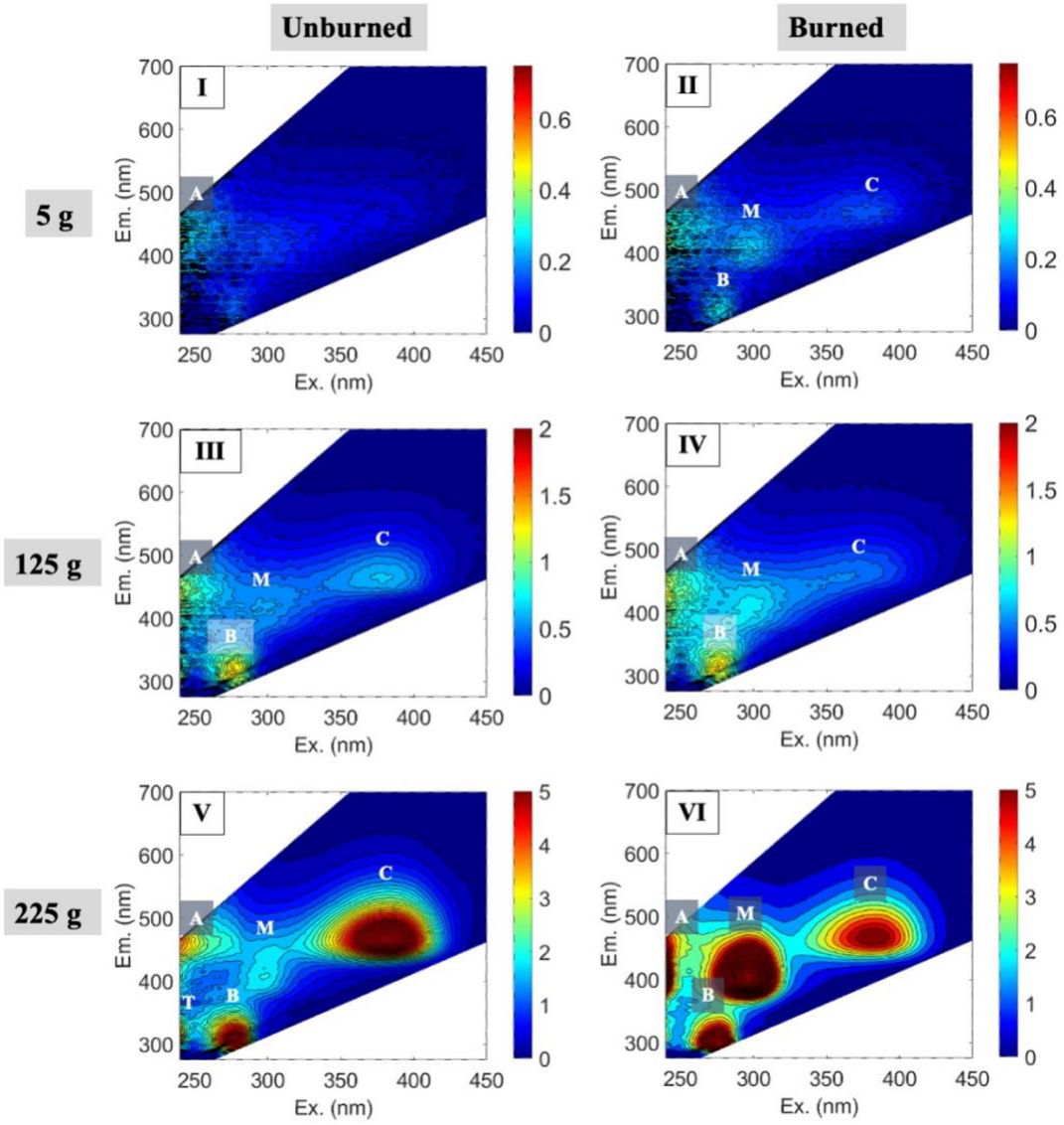

852

853 **Figure S4.** Six Excitation-Emission Matrices (EEMs) showing fluorescence of dissolved organic
854 carbon (DOC) at Day 10: Panel A = 5g, unburned; Panel B = 5g, burned; Panel C = 125g,
855 unburned; Panel D = 125g, burned; Panel E = 225g, unburned; Panel F = 225g, burned. Note, the
856 presence or absence of fluorescence peaks, intensity of fluorescence response, and shifts in peak
857 maxima have all been shown to provide information about DOC chemistry and origin: Peak A
858 (humic-like, λex=~250 nm; λem=380-460 nm), Peak C (humic-like, λex=~405 nm; λem= 490-
859 510 nm), Peak M (protein-like, λex=~312 nm; λem=380-420 nm), and Peak B (protein-like,
860 λex=~275 nm; λem=~310-320 nm).

Fire and browning effects on DOM

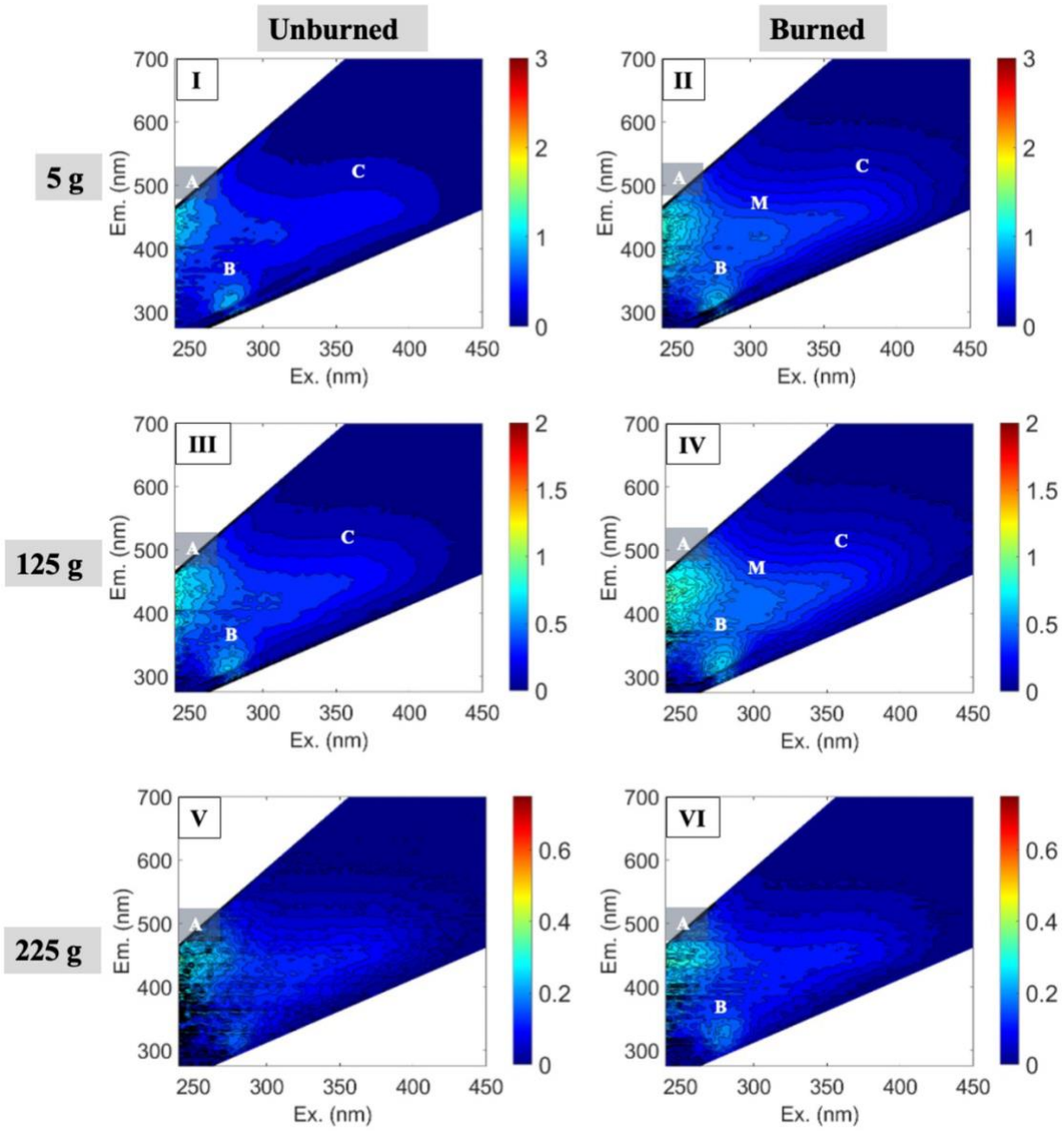

Figure S5. Six Excitation-Emission Matrices (EEMs) showing fluorescence of dissolved organic carbon (DOC) at Day 31: Panel A = 5g, unburned; Panel B = 5g, burned; Panel C = 125g, unburned; Panel D = 125g, burned; Panel E = 225g, unburned; Panel F = 225g, burned. Note, the presence or absence of fluorescence peaks, intensity of fluorescence response, and shifts in peak maxima have all been shown to provide information about DOC character and origin. Peak A (λex=~250 nm; λem=380-460 nm), Peak C (λex=~405 nm; λem= 490-510 nm), Peak M (λex=~312 nm; λem=380-420 nm), and Peak B (λex=~275 nm; λem=~310-320 nm).

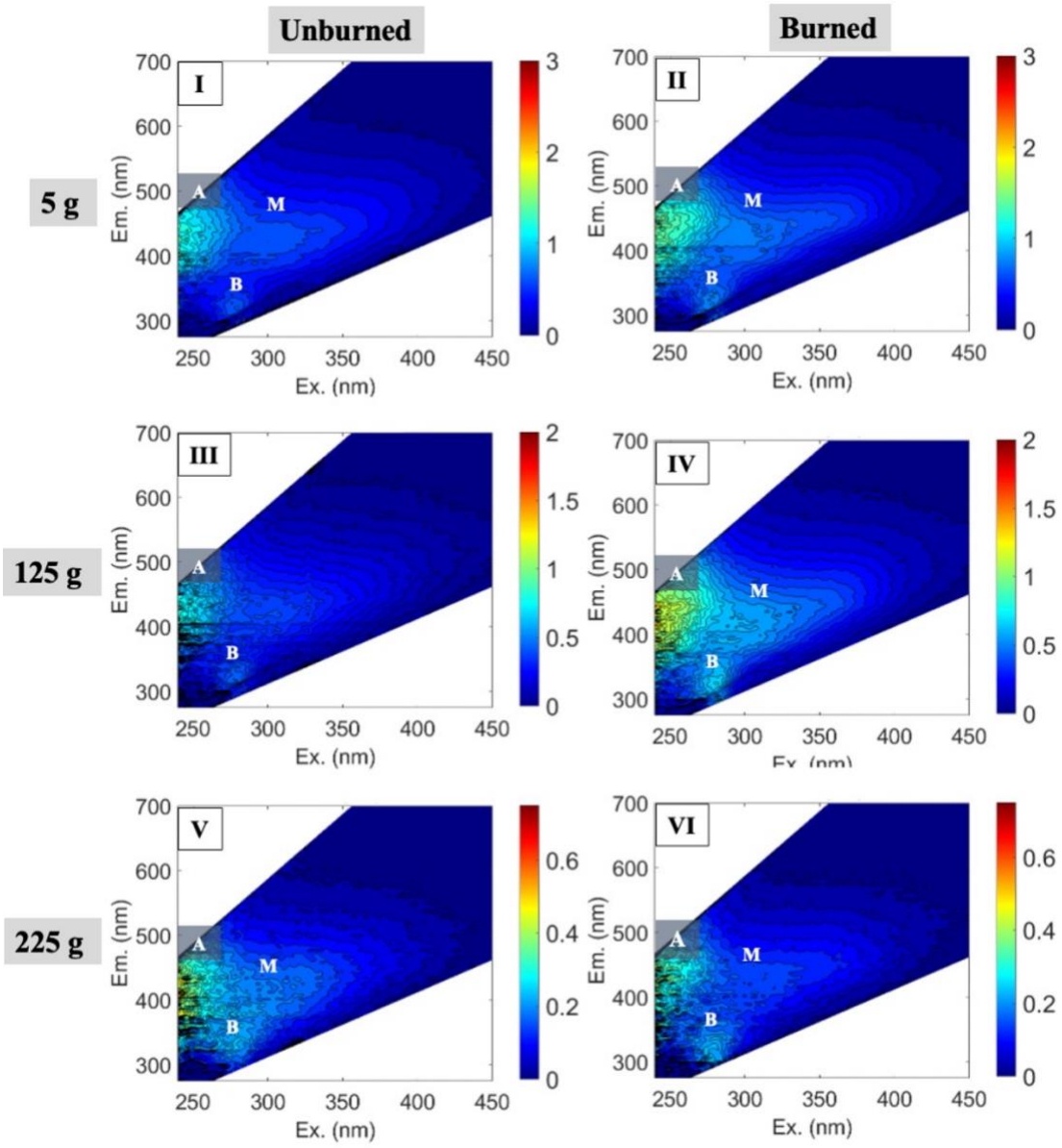

Figure S6. Six Excitation-Emission Matrices (EEMs) showing fluorescence of dissolved organic carbon (DOC) at Day 59: Panel A = 5g, unburned; Panel B = 5g, burned; Panel C = 125g, unburned; Panel D = 125g, burned; Panel E = 225g, unburned; Panel F = 225g, burned. Note, the presence or absence of fluorescence peaks, intensity of fluorescence response, and shifts in peak maxima have all been shown to provide information about DOC character and origin. Peak A (λex=~250 nm; λem=380-460 nm), Peak C (λex=~405 nm; λem= 490-510 nm), Peak M (λex=~312 nm; λem=380-420 nm), and Peak B (λex=~275 nm; λem=~310-320 nm).

Fire and browning effects on DOM

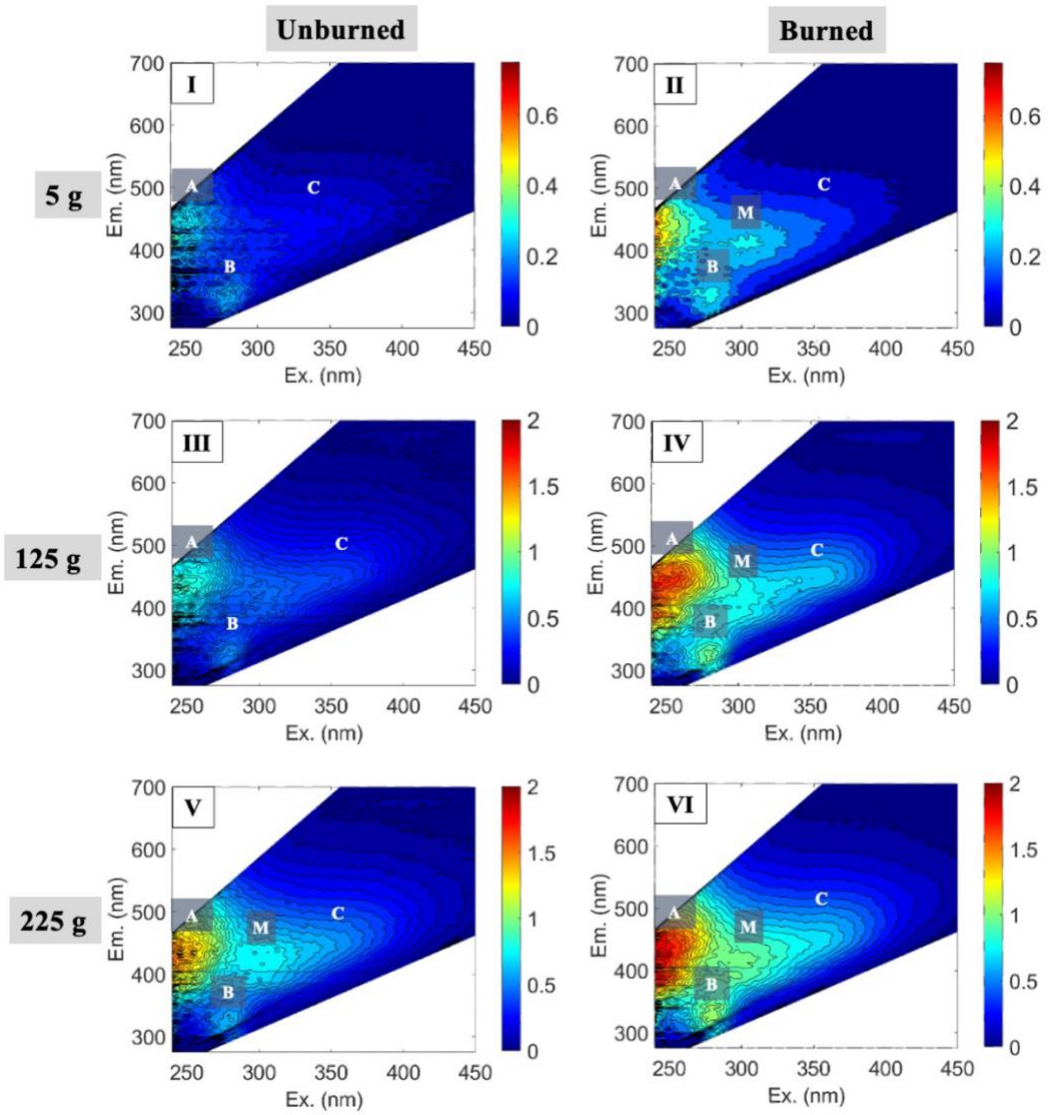

Figure S7. Six Excitation-Emission Matrices (EEMs) showing fluorescence of dissolved organic carbon (DOC) at Day 89: Panel A = 5g, unburned; Panel B = 5g, burned; Panel C = 125g, unburned; Panel D = 125g, burned; Panel E = 225g, unburned; Panel F = 225g, burned. Note, the presence or absence of fluorescence peaks, intensity of fluorescence response, and shifts in peak maxima have all been shown to provide information about DOC character and origin. Peak A (humic-like, λex=~250 nm; λem=380-460 nm), Peak C (humic-like, λex=~405 nm; λem= 490-510 nm), Peak M (protein-like, λex=~312 nm; λem=380-420 nm), and Peak B (protein-like, λex=~275 nm; λem=~310-320 nm).

Fire and browning effects on DOM

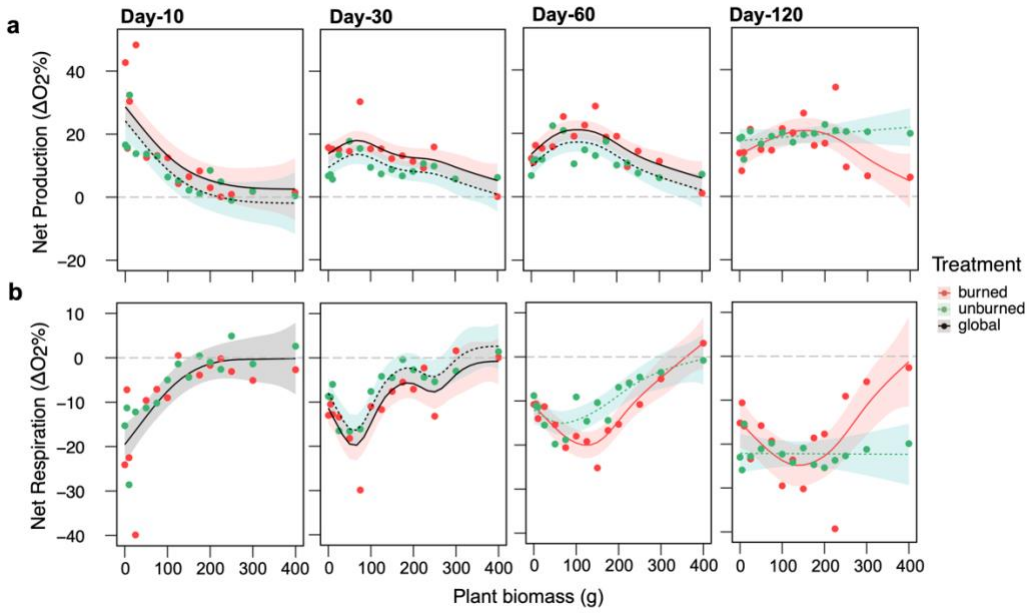

886

887 **Figure S8.** (a) Net ecosystem productivity (NPP) and (b) respiration (R) in treatments receiving burned and

888 unburned plant material across four sampling periods. Plots with a single global smooth indicates that a model

889 with one fit line for the burned and unburned treatments best describes the data, while separate smooths

890 for each fire treatment indicate that a model with different fits for the two burning treatments showed best

891 agreement.